

Contribution from the Departments of Chemistry, Massachusetts Institute of Technology, Cambridge, Massachusetts 02139, and Columbia University, New York, New York 10027

Magnetic, ESR, Electrochemical, and Potentiometric Titration Studies of the Imidazolate-Bridged Dicopper(II) Ion in a Binucleating Macrocyclic

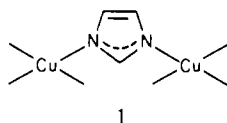
PETER K. COUGHLIN and STEPHEN J. LIPPARD*

Received August 2, 1983

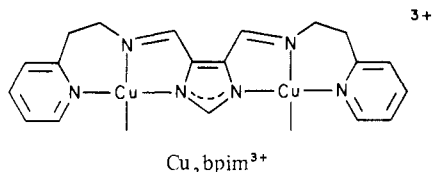
Physical studies of the imidazolate-bridged dicopper(II) ion coordinated to the ligands 1,4,7,13,16,19-hexaaza-10,22-dioxacyclotetracosane (A) and 1,4,7,13,16,19-hexaazacyclotetracosane (A') were carried out to explore the influence of these binucleating macrocycles on the stability of the $\text{Cu}_2(\text{im})^{3+}$ core (imH = imidazole). Temperature-dependent magnetic susceptibility studies of solid $[\text{Cu}_2(\text{im})(\text{imH})_2\text{CA}](\text{ClO}_4)_3$ and $[\text{Cu}_2(\text{im})\text{CA}'](\text{ClO}_4)_3 \cdot \text{H}_2\text{O}$ revealed antiferromagnetic behavior with $J = -27.60$ (7) and -29.40 (3) cm^{-1} , respectively. These values demonstrate that the magnetic interaction between copper(II) centers in the $\text{Cu}_2(\text{im})^{3+}$ ion is unaltered by its coordination to these macrocyclic ligands. The solution properties differed markedly, however. From pH-dependent electron spin resonance and potentiometric titration data it was determined that the imidazolate bridge in $[\text{Cu}_2(\text{im})\text{CA}]^{3+}$ is much more stable than in related complexes such as $[\text{Cu}_2(\text{TMDT})_2(\text{im})]^{3+}$, where TMDT = 1,1,7,7-tetramethyldiethylenetriamine. Equilibrium constants as well as ΔH and ΔS values for the bridge-splitting reactions were determined. Cyclic voltammograms of $[\text{Cu}_2(\text{im})\text{CA}]^{3+}$ in acetonitrile under various conditions showed only irreversible behavior, ascribed to the instability of the cuprous derivatives of the binucleating macrocycle.

Introduction

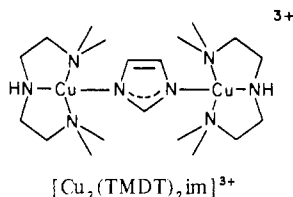
We and others have been interested in imidazolate-bridged dicopper(II) complexes as models for the histidine-bridged bimetallic center (1) in bovine erythrocyte superoxide dis-



mutase (BESOD) and its derivatives.¹ Although the species $\text{Cu}_2\text{im}^{3+}$ (imH = imidazole) is relatively easy to assemble by using tridentate chelating amine and related ligands, solution ESR and potentiometric titration data revealed the imidazolate bridge to be stable only over a narrow pH range, unless it was built into a chelating ligand, as was the case for $\text{Cu}_2\text{bpim}^{3+}$.^{2,3}

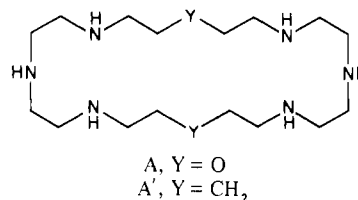


Examination of space-filling models of the structure² of $[\text{Cu}_2(\text{TMDT})_2(\text{im})]^{3+}$, TMDT = 1,1,7,7-tetramethyldi-



ethylenetriamine, revealed that a trimethylene or similar chain would be of sufficient length to link the methyl groups of the two diethylenetriamine poles and still accommodate the $\text{Cu}_2\text{im}^{3+}$ unit. Accordingly, in order to convey the desired aqueous solution stability, binucleating macrocycles 1,4,7,13,16,19-hexaaza-10,22-dioxacyclotetracosane (A) and 1,4,7,13,16,19-hexaazacyclotetracosane (A') were designed and studied as ligands for the imidazolate-bridged dicopper(II) ion.

In this paper we report the results of magnetic, ESR spectroscopic, and potentiometric titrations of the $[\text{Cu}_2(\text{im})\text{CA}]^{3+}$ cation and the magnetic properties of $[\text{Cu}_2(\text{im})\text{CA}]^{3+}$.



$(\text{imH})_2\text{CA}]^{3+}$. The synthesis, structures, and some preliminary results for these complexes as well as $[\text{Cu}_2(\text{im})(\text{MeIm})_2\text{CA}]^{3+}$ (MeIm = 1-methylimidazole) were described previously.⁴ During the course of our investigation, related work on imidazolate-bridged dicopper(II) complexes of binucleating Schiff base macrocycles appeared,⁵ and while this paper was in preparation, a potentiometric equilibrium study of the $[\text{Cu}_2(\text{im})\text{CA}]^{3+}$ cation was published.⁶ From the present results it is clear that the stability of the $\text{Cu}_2\text{im}^{3+}$ ion is significantly enhanced by the presence of the binucleating macrocycles.

Experimental Section

Chemicals and Reagents. 1,4,7,13,16,19-Hexaazacyclotetracosane, macrocycle A', was a gift from A. E. Martin and J. Bulkowski. The complexes $[\text{Cu}_2(\text{im})\text{CA}'](\text{ClO}_4)_3 \cdot \text{H}_2\text{O}$ and $[\text{Cu}_2(\text{im})(\text{imH})_2\text{CA}](\text{ClO}_4)_3$ were prepared as described previously.^{4c} Tetrabutylammonium perchlorate (Eastman) was triply recrystallized from a pentane/ethyl acetate mixture and dried under vacuum at 110 °C. Acetonitrile was distilled from calcium hydride under nitrogen and protected from oxygen and moisture prior to use. For electrochemical work dimethyl sulfoxide, Me_2SO , was distilled under vacuum from barium oxide. Carbonate-free sodium hydroxide was made in the usual way,⁷ standardized with potassium hydrogen phthalate, and protected from carbon dioxide prior to use. Nitric acid was standardized with standard sodium hydroxide and was also protected from carbon dioxide. The

- (1) For a review of the literature, see: Strothkamp, K. G.; Lippard, S. J. *Acc. Chem. Res.* **1982**, *10*, 318.
- (2) O'Young, C.-L.; Dewan, J. C.; Lippard, S. J. *J. Am. Chem. Soc.* **1978**, *100*, 7291.
- (3) Kolks, G.; Frihart, C. R.; Coughlin, P. K.; Lippard, S. J. *Inorg. Chem.* **1981**, *20*, 2933.
- (4) (a) Coughlin, P. K.; Dewan, J. C.; Lippard, S. J.; Watanabe, E.-I.; Lehn, J.-M. *J. Am. Chem. Soc.* **1979**, *101*, 265. (b) Coughlin, P. K.; Lippard, S. J.; Martin, A. E.; Bulkowski, J. E. *Ibid.* **1980**, *102*, 7617. (c) Coughlin, P. K.; Martin, A. E.; Dewan, J. C.; Watanabe, E.-I.; Bulkowski, J. E.; Lehn, J.-M.; Lippard, S. J. *Inorg. Chem.* **1984**, *23*, 1004.
- (5) (a) Cairns, C.; Lavery, A.; Nelson, S. M.; Drew, M. G. B. *J. Chem. Soc., Chem. Commun.* **1980**, 1122. (b) Drew, M. G. B.; McCann, M.; Nelson, S. M. *J. Chem. Soc., Dalton Trans.* **1981**, 1868.
- (6) Motekaitis, R. J.; Martell, A. E.; Lecomte, J.-P.; Lehn, J.-M. *Inorg. Chem.* **1983**, *22*, 609.
- (7) Kolthoff, I. M.; Dandell, E. B.; Melhan, E. J.; Bruckenstein, S. In "Quantitative Chemical Analysis"; MacMillan: New York, 1969.

* To whom correspondence should be addressed at Massachusetts Institute of Technology.

water used was distilled, deionized, and deaerated.

Magnetic Susceptibility Measurements. Variable-temperature magnetic susceptibility measurements were made on powdered samples over the temperature range $4.2 < T < 300$ K by the Faraday method using a locally built susceptometer. The details of the construction and calibration of this instrument are presented elsewhere.⁸ Typically, between 10 and 15 mg of sample were used for the susceptibility determinations. The measurements were started at room temperature, and the sample was cooled and held at the desired temperature during the measurement. This process was continued until the sample was at 4.2 K. The possibility of ferromagnetic impurities was checked by the measurement of the magnetic susceptibility as a function of field strength at various temperatures. None of the compounds tested showed a field dependence of the susceptibility, and therefore no correction for ferromagnetism was needed.

The diamagnetic corrections were made by using Pascal's constants.⁹ The value of the diamagnetic correction for imidazole was measured to be -36.1×10^{-6} cgsu/mol. The value for imidazolate was assumed to be -33.2×10^{-6} cgsu/mol. The theoretical expression was fit to the data by the method of least squares using a locally written program¹⁰ on a VAX 11/780 computer.

Electron Spin Resonance Spectra. Solution spectra were recorded on frozen 1:1 water:Me₂SO solutions that were 5 mM in macrocycle.² The pH reported is the pH measured after the addition of 1 N sodium hydroxide or 1 N nitric acid and before the addition of Me₂SO. The spectra were recorded on a Varian E-line X-band spectrometer equipped with a Varian Model V6040 or Air Products Model LTD-3-110 temperature controller. The magnetic field was calibrated with the manganese impurity in strontium oxide as an external standard.¹¹

Potentiometric Titrations. The pH was measured with a Radiometer TTT-1C pH meter using a combination-glass microelectrode. The meter was calibrated at pH 7 and pH 4 with commercially available buffer solutions, phosphate and phthalate, respectively, taking into account the reported temperature variation in the pH of the solutions.¹² The temperature was controlled with a Lauda K-4/RD circulating temperature controller and jacketed reaction vessel to better than 0.1 °C. The solutions titrated were typically 2.5–3.0 mM in complex and 0.16 M in potassium nitrate, made from carbonate-free deionized water, and were protected from the atmosphere during the titration by bubbling nitrogen through the solution. The nitrogen was saturated with water by passing it through a 0.16 N potassium nitrate solution before it was bubbled into the titration solution. The effect of any evaporation of the solution was corrected for by measurement of the volume of the solution both before and after the titration and by assuming that evaporation, if any, had taken place at a constant rate. The addition of standard acid and base was made with a Gilson 2-mL microliter buret, the tip of which was kept just under the surface of the solution being titrated while the solution was stirred with a magnetic stirrer. The proton number, \bar{P} ,¹³ reported is the average number of protons added to a molecule (when titrating with acid). It was calculated from the known amount of acid that was measured to be free in solution. The programs used to calculate \bar{P} and the equilibrium constants were written locally and are described in ref 8.

Electrochemistry. Cyclic voltammetry studies were performed with a Princeton Applied Research Model 175 universal programmer and a PAR Model 173 potentiostat/galvanostat equipped with a Model 179 coulometer. The voltammograms were recorded with a Houston Instruments Model 2000 X-Y recorder. Temperature control was accomplished as in the potentiometric titrations. For the studies in aqueous solution a commercial saturated calomel electrode, SCE, was used as a reference electrode. For the studies in acetonitrile or Me₂SO the reference electrode was a silver wire in a 0.01 N silver nitrate solution, which was freshly made for each day's use. All the volt-

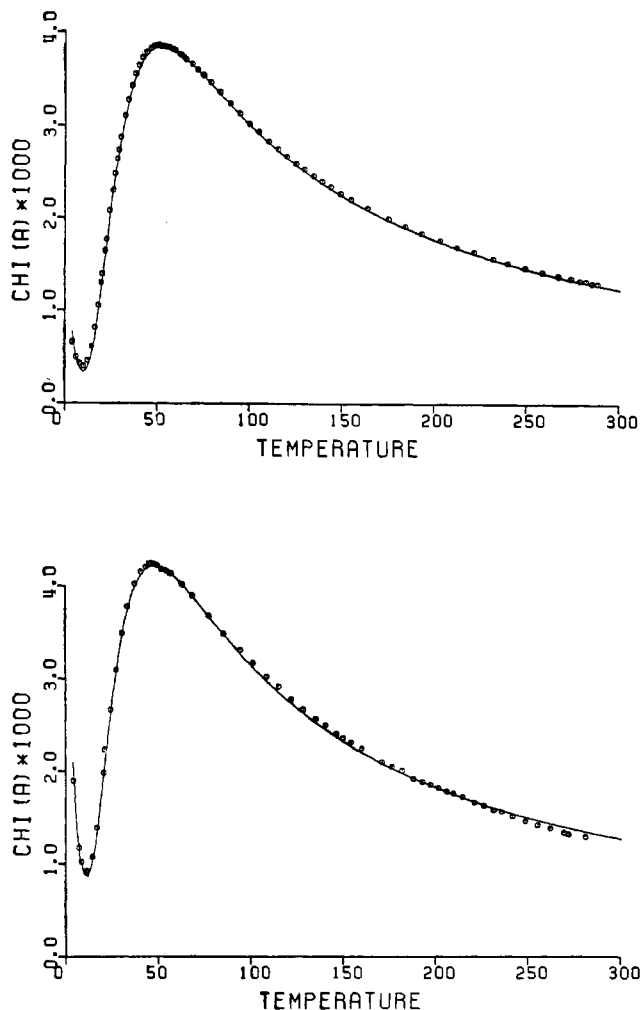


Figure 1. Plot of the corrected atomic susceptibility (cgsu/copper ion) of (top) $[\text{Cu}_2(\text{im})(\text{imH})_2\text{CA}](\text{ClO}_4)_3$ and (bottom) $[\text{Cu}_2(\text{im})\text{CA}'](\text{ClO}_4)_3 \cdot \text{H}_2\text{O}$ as a function of temperature (K). The open circles are the experimental data points. The line is the result of fitting the parameters as described in the text.

ammograms are referenced to the ferrocene/ferrocenium couple, which was used as an external standard in the nonaqueous solutions.¹⁴ The peak-to-peak potential separation, $E_{\text{pa}} - E_{\text{pc}}$, of this couple was used to check the system for uncompensated resistance since it is known to be reversible in the solvents used. The couple, which was assumed to have a value of +0.4000 V vs. aqueous SCE, has been reported to have a redox potential that is solvent independent.¹⁴ The working electrodes were locally constructed platinum-bead or glassy-carbon electrodes. The counterelectrode was a platinum wire. The solutions were ~0.5 mM in complex and 0.1 M in supporting electrolyte, potassium nitrate for aqueous solutions and tetrabutylammonium perchlorate for nonaqueous solutions. Dry nitrogen was bubbled through the solution prior to electrolysis and blanketed the solution while the voltammograms were recorded.

Results and Discussion

Magnetic Exchange through the Imidazolate Bridge. Plots of magnetic susceptibility vs. temperature for solid $[\text{Cu}_2(\text{im})(\text{imH})_2\text{CA}](\text{ClO}_4)_3$ and $[\text{Cu}_2(\text{im})\text{CA}'](\text{ClO}_4)_3 \cdot \text{H}_2\text{O}$ are shown in Figure 1. Both curves exhibit maxima indicative of antiferromagnetic coupling. As the temperature is lowered from that of the maximum, the susceptibility becomes a minimum and then rises again. The low-temperature tail is due to a small amount (~1%) of paramagnetic impurity in the sample. Fitting the data to the Bleaney-Bowers equation,¹⁵

- (8) Coughlin, P. K. Ph.D. dissertation, Columbia University, 1981.
- (9) Figgis, B. N.; Lewis, J. In "Modern Coordination Chemistry"; Lewis, J., Wilkins, R. G., Eds.; Interscience: New York, 1960.
- (10) Karlin, K. Ph.D. Dissertation, Columbia University, 1975.
- (11) Bolton, J. R.; Borg, D. C.; Swartz, H. M. in "Biological Applications of Electron Spin Resonance"; Swartz, H. M., Bolton, J. R., Borg, D. C., Eds.; Interscience: New York, 1972.
- (12) "CRC Handbook of Chemistry and Physics", 54th Ed.; CRC Press: Cleveland, 1973; p D112.
- (13) Anderegg, G. In "Coordination Chemistry"; Martell, A. E., Ed.; American Chemical Society: Washington, DC 1971; ACS Monogr. No. 168.

- (14) (a) Koepp, H. M.; Wendt, H.; Strehlow, H. Z. *Elektrochem.* **1960**, *64*, 438. (b) Bauer, D.; Breat, M. In "Electroanalytical Chemistry"; Bard, A. J., Ed.; Marcel Dekker: New York, 1975; Vol. 8.

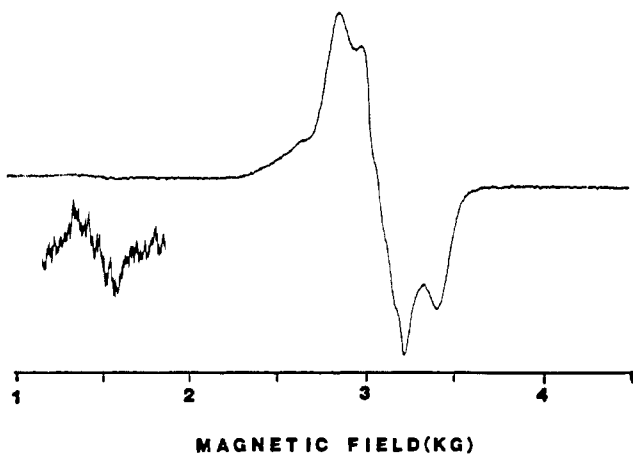


Figure 2. ESR spectrum of $[\text{Cu}_2(\text{im})\text{CA}'](\text{ClO}_4)_3 \cdot \text{H}_2\text{O}$ in frozen 50% aqueous Me_2SO at 77 K. The $\Delta M_S = \pm 2$ region ~ 1500 G is magnified $\times 20$.

modified to account for paramagnetic impurities and temperature-independent paramagnetism in the manner described previously,¹⁶ gave $J = -27.60$ (7) cm^{-1} and $g = 2.10$ (1) for $[\text{Cu}_2(\text{im})(\text{imH})_2\text{CA}'](\text{ClO}_4)_3$ and $J = -29.40$ (3) cm^{-1} and $g = 2.077$ (1) for $[\text{Cu}_2(\text{im})\text{CA}'](\text{ClO}_4)_3 \cdot \text{H}_2\text{O}$. Observed and calculated molar susceptibilities and effective magnetic moments are reported in Tables S1-S2.¹⁷

The values of the spin exchange coupling constants are typical of imidazolate-bridged dicopper(II) complexes. Mediation of magnetic exchange through the imidazolate anion has been the subject of extensive study.^{16,18} Antiferromagnetic behavior occurs when the $\text{Cu}-\text{im}-\text{Cu}^{3+}$ linkage connects the two copper(II) coordination spheres at axial sites of two trigonal bipyramids, the known structure of $[\text{Cu}_2(\text{im})(\text{imH})_2\text{CA}'](\text{ClO}_4)_3$, or through in-plane sites of two square-planar units, the postulated structure of $[\text{Cu}_2(\text{im})\text{CA}'](\text{ClO}_4)_3 \cdot \text{H}_2\text{O}$.^{4c} The presence of the binucleating macrocycle does not significantly modify the J value, which may be compared with $J = -25.80$ (16) cm^{-1} for $[\text{Cu}_2(\text{TMDT})_2(\text{im})]^{3+2}$ and $J = -27$ cm^{-1} for $[\text{Cu}_2(\text{PMDT})_2(\text{im})]^{3+}$.¹⁸ In the case of $[\text{Cu}_2(\text{im})\text{CA}'](\text{ClO}_4)_3 \cdot \text{H}_2\text{O}$, the magnetic susceptibility results confirm that the structure of this complex has an imidazolate-bridged dicopper(II) core, since X-ray crystallographic verification of this feature could not be achieved owing to poor crystal quality.^{4c}

Also indicative of the $\text{Cu}_2(\text{im})^{3+}$ unit is the frozen-solution electron spin resonance (ESR) spectrum of $[\text{Cu}_2(\text{im})\text{CA}'](\text{ClO}_4)_3 \cdot \text{H}_2\text{O}$, shown in Figure 2. This spectrum, which is markedly different from that of a mononuclear copper(II) complex,¹⁹ exhibits both the $\Delta M_S = \pm 2$ transition at half-field and the high-field feature at " $g_{\text{eff}} \sim 1.9$ " that are characteristic of the imidazolate-bridged dicopper(II) core.^{1,2,16} A qualitative analysis⁸ of the $\Delta M_S = \pm 1$ region of the spectrum in terms of zero-field splitting gave an estimate of 27 cm^{-1} for $|J|$, which is comparable to the value measured by magnetic susceptibility, $|J| = 29.4$ cm^{-1} . In terms of this analysis, the high-field (" $g = 1.9$ ") absorbance previously employed to monitor the stability of the imidazolate bridge in solution^{2,16} is assigned to the parallel component, H_z , of the zero-field splitting. This feature occurs in a spectral region that not only is unusual for an absorbance due to mononuclear copper, as is the $\Delta M_S = \pm 2$

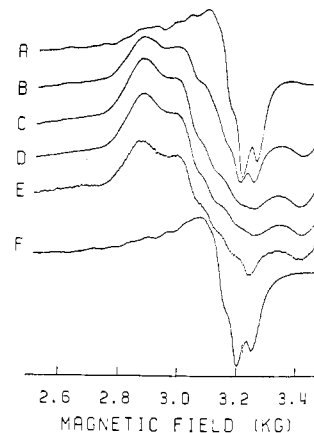


Figure 3. ESR spectra of ~ 5 mM $[\text{Cu}_2(\text{im})\text{CA}']^{3+}$ in frozen (115 K) aqueous Me_2SO where the pH of the aqueous solution before the addition of Me_2SO was (A) 5.6, (B) 6.2, (C) 7.1, (D) 10.4, and (E) 11.5. (F) shows the ESR spectrum of a 2:1 $\text{Cu}(\text{II})$:macrocycle solution, 10 mM in $\text{Cu}(\text{II})$, in 50% aqueous Me_2SO at 77 K.

transition, but also is an unusual region for any absorbance due to any of the normal contaminants of copper. This fact makes the absorbance at " $g = 1.9$ ", i.e. the high-field H_z , even more definitive than the $\Delta M_S = \pm 2$ transition as a measure of the amount of imidazolate bridging.

Solution Stability of the $\text{Cu}_2(\text{im})^{3+}$ Unit in Binucleating Macrocycles. The ESR spectra of $[\text{Cu}_2(\text{im})\text{CA}'](\text{ClO}_4)_3$, measured in the $\Delta M_S = \pm 1$ region as a function of pH in frozen aqueous Me_2SO solutions, are shown in Figure 3. The similarity in spectra B-E indicates that the imidazolate bridge is intact over the pH range 6.2-11.5. The feature at " $g = 1.9$ " remains approximately equal in intensity to the feature at $g = 2.0$ in all the high-pH, $\text{pH} > 7$, spectra. The spectrum of the complex at pH 6.2 (Figure 3B), while being generally similar to the spectra of the complex at high pH, is noticeably different from the others. The feature at " $g = 1.9$ " is diminished in comparison with the feature at $g = 2.0$, which itself has sharpened. The " $g = 1.9$ " signal, while weaker, is definitely present, indicating that much of the copper is still in the form of imidazolate-bridged complex. The pH 5.6 (Figure 3A) spectrum exhibits even more dramatic changes. The feature at " $g = 1.9$ " is almost completely gone, which means that hardly any of the copper is in the form of an imidazolate-bridged complex, and the spectrum looks very much like that of mononuclear copper. The g_{\parallel} region of the spectrum between ~ 2600 and ~ 3100 G is very difficult to interpret, partly due to the overlap of the low-field H_{xy} and H_z features of the small percentage of the remaining binuclear copper. It also appears that the two copper atoms are inequivalent. For equivalent copper ions, the g_{\parallel} region should contain four evenly spaced lines.²⁰ The multiple features in the perpendicular region, $g \sim 2.0$, could be due either to a rhombic distortion of the complex, i.e. anisotropy in the $x-y$ plane, or to overlap of the parallel and perpendicular components of the spectrum. The spectrum in Figure 3F, which is that of a solution of two cupric ions and the macrocycle, can help explain the spectrum of the imidazolate-bridged compound at pH 5.6. While the structure of the complex or complexes formed is unknown, presumably the copper ions are bound to the diethylenetriamine portions of the macrocycle with water molecules coordinated to the fourth sites. The spectrum, which is also very hard to analyze in detail, looks remarkably similar to the spectrum of the imidazolate-bridged complex at pH 5.6. The features match well except in the regions where the imidazolate-bridged species has its maxima and minima. At pH 5.6, therefore, the

(15) Bleaney, B.; Bowers, K. D. *Proc. R. Soc. London, Ser. A* **1952**, 214, 451.

(16) Kolks, G.; Lippard, S. J.; Waszczak, J. V.; Lienthal, H. R. *J. Am. Chem. Soc.* **1982**, 104, 717.

(17) Supplementary material.

(18) (a) Haddad, M. S.; Hendrickson, D. N. *Inorg. Chem.* **1978**, 17, 2622.

(b) Haddad, M. S.; Duesler, E. N.; Hendrickson, D. N. *Ibid.* **1979**, 18, 141.

(19) Peisach, J.; Blumberg, W. E. *Arch. Biochem. Biophys.* **1974**, 165, 691.

(20) Wertz, J. E.; Bolton, J. R. "Electron Spin Resonance Elementary Theory and Practical Applications"; McGraw-Hill: New York, 1972.

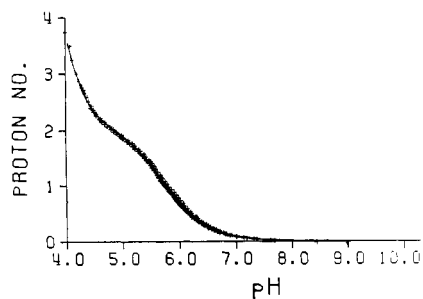
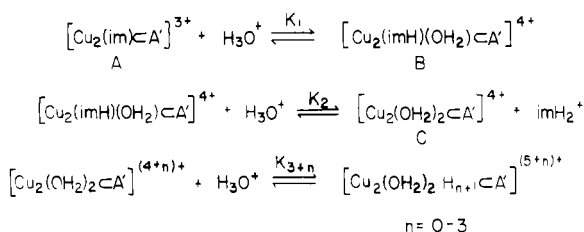


Figure 4. Plot of the titration of $[\text{Cu}_2(\text{im})\text{CA}']^{3+}$. The + signs are the experimental points of both the forward and back titrations. The solid line is the result of the least-squares fitting (see text).



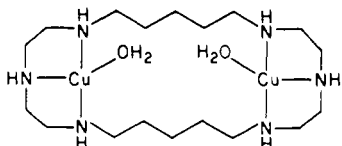
$$K_1 = 1.95 \times 10^5; K_2 = 2.09 \times 10^3; K_3 = K_4 = 9.33 \times 10^3; K_5 = K_6 = 7.94 \times 10^3$$

Figure 5. Equilibria involved in the titration of $[\text{Cu}_2(\text{im})\text{CA}']^{3+}$.

Table I. Equilibrium Constants at Three Temperatures for the Reactions Depicted in Figure 5

	10 °C	25 °C	37.5 °C
K_1	$6.72 (25) \times 10^5$	$1.91 (18) \times 10^5$	$5.4 (19) \times 10^4$
K_2	$3.89 (18) \times 10^2$	$2.06 (21) \times 10^3$	$7.3 (25) \times 10^3$
$K_3 = K_4$	$9.00 (26) \times 10^3$	$9.3 (3) \times 10^3$	$1.10 (4) \times 10^4$
$K_5 = K_6$	$1.12 (9) \times 10^4$	$7.9 (9) \times 10^3$	$4.9 (9) \times 10^3$

imidazolate-bridged complex should mostly consist of a structure without a coordinated imidazole, as shown by



A more quantitative measure of the species present in solution was obtained by potentiometric titration of $[\text{Cu}_2(\text{im})\text{CA}']^{3+}$. Data for the titration of $[\text{Cu}_2(\text{im})\text{CA}']^{3+}$ are shown in Figure 4. As the pH is lowered from 7, the molecule picks up protons from solution. The first two protons titrate quite apart from the rest. These should be the ones involved in breaking the imidazolate bridge. The equilibria involved (Figure 5) are similar to those found for imidazolate-bridged dicopper(II) complexes with both tridentate³ and hexadentate binucleating macrocyclic⁶ amine ligands. The first proton taken up by the complex breaks the bridge to give a coordinated water molecule on one copper ion and a coordinated imidazole on the other. The second proton addition releases imidazolium ion and results in coordinated water molecules on both copper ions. Protonation of the amine nitrogen atoms of the macrocycle occurs upon further addition of acid down to pH 4. The potentiometric data were nicely fit by a model in which it was assumed that $K_3 = K_4 \neq K_5 = K_6$ (Figure 5).⁸

The equilibrium constants obtained by least-squares fitting of observed and calculated potentiometric data (see Figure 4) are given in Table I. The value of 5.29 (5) for $\log K_1$ at 25 °C indicates the imidazolate-bridged complex to be very stable, especially above pH 7. The corresponding value for the $[\text{Cu}_2(\text{im})\text{CA}']^{3+}$ system, $\log K_1 = 3.86$ (5), shows this complex to be even more stable.⁶ For both macrocycles A and A' the imidazolate-bridged bimetallic center is substantially more

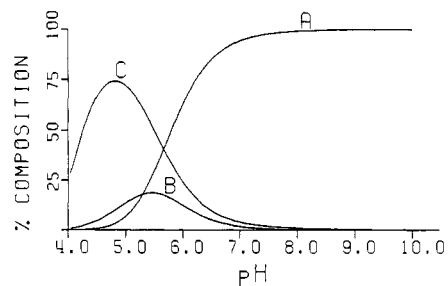


Figure 6. Plot of the relative concentrations of $[\text{Cu}_2(\text{im})\text{CA}']^{3+}$ (A), $[\text{Cu}_2(\text{imH})(\text{OH}_2)\text{CA}']^{4+}$ (B), and $[\text{Cu}_2(\text{OH}_2)_2\text{CA}']^{4+}$ (C) as a function of pH for an aqueous solution of $[\text{Cu}_2(\text{im})\text{CA}']^{3+}$, 5 mM in macrocycle. Species containing protonated macrocycle are omitted from the plot for clarity.

robust than for nonmacrocyclic complexes previously studied^{2,3} or for the imidazolate-bridged methylmercury system.²¹ The $\log K_2$ value of 3.32 can be converted into a formation constant for the reaction of imidazole with the dicopper macrocycle. This constant, $\log K_f = 3.80$, agrees exactly with the corresponding value for the formation of $[\text{Cu}_2(\text{imH})\text{CA}']^{3+}$ ⁶ and may be compared with results for imidazole binding to the aqueous copper(II) ion, $\log K_1 = 4.33$ and $\log K_2 = 3.27$.²²

From the equilibrium constants may be calculated the concentration of various species in solution as a function of pH at some total concentration of complex. The results of such a calculation for a 5 mM solution of $[\text{Cu}_2(\text{im})\text{CA}']^{3+}$, the concentration at which the ESR spectra were run, are shown in Figure 6. The distribution of species compares closely with that deduced from the ESR titration study. Above pH 7 the bridged species, A (Figure 5), clearly dominates, at pH 6.2 approximately 75% of the copper is in the form of the bridged species, and at pH 5.6 the dominant species (C) is the one with water coordinated to the fourth sites of both copper ions, with a small amount of bridged complex also present. The derived equilibrium constants therefore predict the same species as seen in the ESR spectra of aqueous Me_2SO solutions at corresponding "pH" values. Apparently the cosolvent does not alter appreciably the aqueous solution equilibrium species distribution. Complex B never becomes dominant in solution at a total copper concentration of 5 mM (Figure 4 and 6). Higher total concentrations of copper or excess imidazole could make it an important species over a narrow pH range. These results contrast significantly with those obtained for $[\text{Cu}_2(\text{im})\text{-(TMDT)}_2]^{3+}$.² It is thus apparent that the simple idea of "tying" together the two diethylenetriamine units into a macrocycle in order to stabilize the imidazolate bridge in solution has worked remarkably well.

In order to investigate the thermodynamic basis for the increased stability of the imidazolate bridge in this macrocyclic system, potentiometric titrations were performed at several temperatures. The rationale behind the idea of linking the two diethylenetriamine units in a macrocycle was that bridge breaking would be less favorable entropically. It was therefore of interest to get a direct measure of ΔS for this process. Titrations over the range $10 \leq T \leq 37.5$ °C were used to compute equilibrium constants (Table I), and from eq 1 were

$$\ln K = \Delta S/R - \Delta H/RT \quad (1)$$

calculated ΔS and ΔH for equilibria 1 and 2 by a least-squares fit to the data. Plots of $\ln K$ vs. T^{-1} for the data and the least-squares line for K_1 and K_2 are given in ref 8. The derived thermodynamic constants are $\Delta H_1 = -16.7$ kcal mol⁻¹, ΔS_1

(21) Evans, C. A.; Rabenstein, D. L.; Geier, G.; Erni, I. W. *J. Am. Chem. Soc.* **1977**, *99*, 8106.

(22) Sklenskaya, E. V.; Karapet'Yants, M. Kh. *Russ. J. Inorg. Chem. (Engl. Transl.)* **1966**, *11*, 1102 (2061).

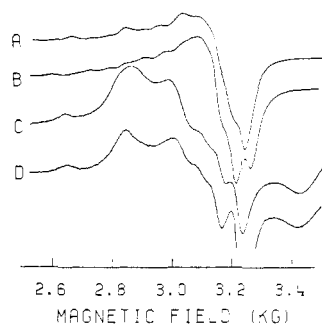
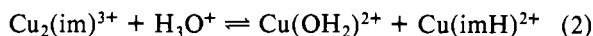


Figure 7. ESR spectra of frozen (77 K) aqueous Me_2SO solutions of $\text{Cu}:\text{A}':\text{imH}:\text{H}^+$ in the ratios of (A) 1:1:0:0, (B) 2:1:0:0, (C) 1:1:1:0, and (D) 1:1:1:1. All solutions were ~ 5 mM in macrocycle.

$= -32$ eu, $\Delta H_2 = 18.7$ kcal mol $^{-1}$, and $\Delta S_2 = 77.8$ eu. From the sign and magnitude of these values it is possible to understand how the macrocycle has such a stabilizing effect on the $\text{Cu}_2(\text{im})^{3+}$ ion. The ΔS for the bridge breaking is -32 eu. This negative value is consistent with an equilibrium process in which two species in solutions become one, viz., $\text{A} + \text{H}_3\text{O}^+ \rightleftharpoons \text{B}$ (Figure 5). In nonmacrocylic complexes the corresponding equilibrium would be given by eq 2, for which ΔS



would be much less negative. Although there are no thermodynamic data available for reactions such as eq 2, the entropy changes for hydroxide-bridged species breaking up to hydrated cations are quite large, $\sim +50$ eu.²³ Clearly the bridge-splitting reaction becomes entropically much less favorable when the imidazolate-bridged dicopper(II) unit is bound to a binucleating macrocycle.

The large entropic change, $\Delta S = +78$ eu, for the second equilibrium is a little hard to explain. The exchange of a coordinated imidazole for a coordinated water molecule should have a small positive entropy change.²² Imidazole going to imidazolium has an entropy change of $\Delta S = +10$ eu.²⁴ These do not seem to add up to the measured value. It is unlikely that the equilibrium as written is wrong, especially since an independent study with macrocycle A gave the same results.⁶ A possible explanation for the large positive entropy change is that the imidazole ligand in species B is hydrogen bonded to a coordinated water molecule on the adjacent copper center and that this interaction restricts the conformational flexibility of the macrocycle. Release of this constraint would accompany loss of imH_2^+ , contributing to the positive entropy change.

The ΔH values for equilibria 1 and 2, -17 and $+19$ kcal/mol, respectively, are consistent with the expected trends $-\Delta H_f(\text{Cu}-(\text{im})\text{Cu}) < -\Delta H_f(\text{Cu}-\text{imH})$ and $-\Delta H_f(\text{Cu}(\text{im})-\text{H}) > -\Delta H_f(\text{H}-\text{imH})$. Again there are few thermodynamic data to which these values can be directly compared.

The potentiometric titrations show that the imidazolate-bridged species is remarkably stable; even hydroxide, which forms a very stable bridged complex^{6,25} $[\text{Cu}_2(\text{OH})\text{CA}]^{3+}$, cannot compete with imidazolate. Another experiment, that underscores this stability, was carried out in which the ESR spectra were taken of frozen aqueous Me_2SO solutions containing various ratios of copper:macrocycle:imidazole:protons. The results are shown in Figure 7. The spectrum of a solution of copper:macrocycle in a 1:1 ratio (Figure 7B) is significantly different from the spectrum of the 2:1 ratio of copper to macrocycle (Figure 7A). The 1:1 solution seems to contain more than one species, as evident from the g_{\parallel} region of the

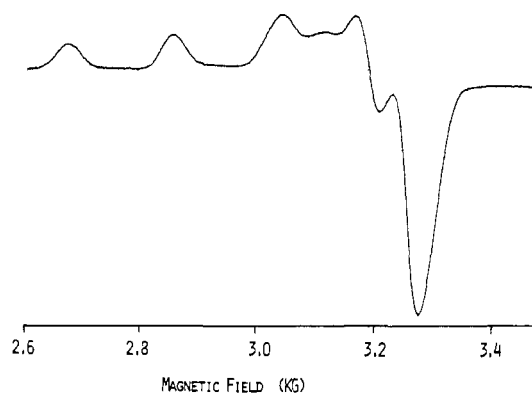


Figure 8. ESR spectrum of a frozen (120 K) aqueous Me_2SO solution of $\text{Cu}:\text{dien}:\text{imH}$ in the ratio 1:2:1 with a copper concentration of ~ 5 mM.

Table II. Cyclic Voltammetry Results at the Glassy-Carbon Electrode^a

compd	solvent ^b	E_{R_1} ^c	E_{R_2} ^c	E_{O_1} ^d	E_{O_2} ^d
$[\text{Cu}_2(\text{im})\text{CA}]^{3+}$	ACN	-884	-986	-287	
	ACN + 1% H_2O	-890	-995	-290	
	ACN + 2% H_2O		-1063	-230	
	H_2O	-726	-912	-446	
	Me_2SO		-985	-245	-705
$(\text{Cu}_2\text{CA})^{4+}$	ACN	-703	-900	-185	
$(\text{Cu}_2\text{CA})^{4+} + \text{MeIm}$	ACN		-937	-274	
$(\text{Cu}_2\text{CA})^{4+} + 2\text{MeIm}$	ACN		-900	-361	

^a All potentials are reported in mV vs. the Fc/Fc^+ couple.

^b ACN, acetonitrile; Me_2SO , dimethyl sulfoxide. ^c Peak potential for reduction. ^d Peak potential for oxidation.

spectrum, although none of these species corresponds to those in the solution with the 2:1 copper:macrocycle ratio. This result shows that, when $\text{Cu}:\text{A}$ is 1:1, very little if any $[\text{Cu}_2\text{CA}]^{3+}$ exists. This conclusion is in good accord with potentiometric equilibrium results for 1:1 copper(II):A solutions.⁶ When imidazole is added to the solution, however, the ESR spectrum (Figure 7C) reveals that a large percentage of the copper is imidazolate bridged. The spectrum is similar to that of the $[\text{Cu}_2(\text{im})\text{CA}]^{3+}$ ion at pH 6.2 (Figure 3B). Under similar conditions, in the nonmacrocylic system $\text{Cu}:\text{dien}:\text{imH}$ of 1:2:1, there is no hint of an imidazolate-bridged species, as can be seen in Figure 8. These results clearly show that at $\text{Cu}:\text{A}':\text{imH}$ ratios of 1:1:1 the copper ions are in the same macrocycle in the form of the imidazolate-bridged species $[\text{Cu}_2(\text{im})\text{CA}]^{3+}$, with remaining macrocycles and imidazoles free to pick up the protons released in forming the imidazolate bridge. This stable imidazolate-bridged complex forms even when imidazolium is added to the system instead of imidazole, as can be seen in Figure 7D. The amount of bridged species is less but still significant. The migration of both metals to the same macrocycle in the presence of imidazole is related to a property of the superoxide dismutase system, as discussed below.

Electrochemistry. The results of cyclic voltammetric experiments are given in Table II. The copper(II) in $[\text{Cu}_2(\text{im})\text{CA}]^{3+}$ reduces in two irreversible steps, indicating that the copper atoms are interacting sufficiently to make them inequivalent, unlike the imidazolate-bridged nonmacrocylic cases where the copper atoms are electrochemically equivalent.²⁶ When the system was left at a potential slightly more negative than the second reduction potential, the copper(I) disproportionated to copper(II) and copper metal, which plated out onto the electrode. The instability of the cuprous form of the complex obviates any comparisons of these results with

(23) Smith, R. M.; Martell, A. E. "Critical Stability Constants"; Plenum Press: New York, 1976; Vol. 4.

(24) Datta, S. P.; Grzybowski, J. *J. Chem. Soc. A* **1966**, 1059.

(25) Coughlin, P. K.; Lippard, S. J. *J. Am. Chem. Soc.* **1981**, *103*, 3328.

(26) O'Young, C.-L. Ph.D. Dissertation, Columbia University, 1980.

those of the enzyme BESOD.

The potential of the reduction is not strongly dependent upon solvent, indicating that the initial and reduced species are interacting with the solvent in a similar manner. The reoxidation wave depends on many variables, however. Its solvent dependence shows that one of the species involved in this redox process interacts more strongly with the solvent than does the other. Reoxidation of the unbridged complex in the presence of 1 equiv of added 1-methylimidazole is similar to reoxidation of the bridged species. Moreover, the relative current of the reoxidation increases upon addition of water. These results suggest that the complex being reoxidized following reduction of $[\text{Cu}_2(\text{im})\text{CA}]^{3+}$ might be a species with the imidazolate bridge broken.

Comparisons with BESOD. The original purpose for synthesizing imidazolate-bridged complexes was to study them as models for the active site of the enzyme BESOD.¹ The first discrete imidazolate-bridged complexes, using bpim as the source of imidazolate,³ had magnetic and structural properties different from those of the four-copper form of the enzyme.¹⁶ The next generation of imidazolate-bridged complexes, using simple tridentate ligands for the copper and imidazolate, had magnetic properties similar to those of the enzyme, but the imidazolate bridge was never 100% intact in solution and was only a major species in solution over a narrow pH range.² The macrocycles provide a very stable environment for the $\text{Cu}_2(\text{im})^{3+}$ ion. It remains intact over a wide pH range, exhibiting a stability similar to that of the imidazolate bridge in the enzyme. The magnetic properties of $[\text{Cu}_2(\text{im})(\text{imH})_2\text{CA}]^{3+}$ and $[\text{Cu}_2(\text{im})\text{CA}]^{3+}$ also match those of $\text{Cu}_2\text{Cu}_2\text{SOD}$.

The form of the enzyme with copper in the copper site and nothing in the zinc site, $\text{Cu}_2\text{E}_2\text{BESOD}$, has an unusual pH-dependent metal migration²⁷ for which some of the chemistry reported here is a good model. At neutral pH the ESR

spectrum of $\text{Cu}_2\text{E}_2\text{SOD}$ resembles that of mononuclear copper, as expected since each copper ion is in a separate subunit. As the pH is raised, the ESR spectrum changes from that of mononuclear copper to a spectrum similar to that of $\text{Cu}_2\text{Cu}_2\text{SOD}$. The copper ions migrate to form an imidazolate-bridged dicopper(II) unit in a single subunit. This behavior was also observed in solutions of copper:macrocycle:imidazole in 1:1:1 ratios.

One area in which the macrocyclic complex is less satisfactory as a model for BESOD or $\text{Cu}_2\text{Cu}_2\text{SOD}$ involves the redox chemistry of the copper ions. The redox potential of the copper in native BESOD is much more positive than the potential in the macrocyclic complex. The high redox potential of the enzyme is probably due to the tetrahedral distortion of the copper site revealed in the high-resolution X-ray crystal structure of BESOD.²⁸ Additional comparisons of the properties of $[\text{Cu}_2(\text{im})\text{CA}]^{3+}$ and $[\text{Cu}_2(\text{im})(\text{imH})_2\text{CA}]^{3+}$ with those of superoxide dismutase and its derivatives are given elsewhere.¹

Acknowledgment. This work was supported by research grants from the National Science Foundation and the National Institute of General Medical Sciences, NIH. We thank J. V. Plust for technical assistance. We also thank Drs. A. E. Martin and J. Bulkowski for providing a generous amount of the ligand A'.

Registry No. $[\text{Cu}_2(\text{im})(\text{imH})_2\text{CA}](\text{ClO}_4)_3$, 69470-57-1; $[\text{Cu}_2(\text{im})\text{CA}](\text{ClO}_4)_3$, 76096-70-3; $[\text{Cu}_2(\text{im})(\text{imH})_2\text{CA}]^{3+}$, 69470-56-0; $[\text{Cu}_2(\text{im})\text{CA}]^{3+}$, 76096-69-0.

Supplementary Material Available: Tables S1 and S2 listing observed and calculated molar susceptibilities and magnetic moments vs. temperature for $[\text{Cu}_2(\text{im})(\text{imH})_2\text{CA}](\text{ClO}_4)_3$ and $[\text{Cu}_2(\text{im})\text{CA}](\text{ClO}_4)_3 \cdot \text{H}_2\text{O}$, respectively (5 pages). Ordering information is given on any current masthead page.

(27) Valentine, J. S.; Pantoliano, M. W.; McDonnell, P. J.; Burger, A. R.; Lippard, S. J. *Proc. Natl. Acad. Sci. U.S.A.* **1979**, *76*, 4245.

(28) Tainer, J. A.; Getzoff, E. D.; Beem, K. M.; Richardson, J. S.; Richardson, D. C. *J. Mol. Biol.* **1982**, *160*, 181.

Contribution from the Department of Chemistry,
University of Houston, Houston, Texas 77004

Electron-Transfer and Ligand-Addition Reactions of (TPP)Mn(NO) and (TPP)Co(NO) in Nonaqueous Media

S. KELLY, D. LANÇON, and K. M. KADISH*

Received September 19, 1983

The electron-transfer and ligand-addition reactions of the manganese and cobalt porphyrin complexes (TPP)Mn(NO) and (TPP)Co(NO) were studied in nine nonaqueous solvents. In all solvents, stable complexes of $[(\text{TPP})\text{Co}(\text{NO})]^-$, $[(\text{TPP})\text{Co}(\text{NO})]^+$, $[(\text{TPP})\text{Mn}(\text{NO})]^-$, and $[(\text{TPP})\text{Mn}(\text{NO})]^{2-}$ could be generated at the electrode surface. In contrast, $[(\text{TPP})\text{Mn}(\text{NO})]^+$ was not stable and rapidly decomposed to yield $[(\text{TPP})\text{Mn}]^+$ and NO. Spectrophotometric and electrochemical studies in mixed-solvent systems provide clear evidence for the presence of $[(\text{TPP})\text{Co}(\text{NO})(\text{L})]^+$ and (TPP)Mn(NO)(L) in solution, where L = DMF, Me_2SO , and pyridine, and stepwise formation constants for the addition of these ligands are determined. Finally, comparisons are made between the electrochemical stability of (TPP)M(NO) and the metal-nitrosyl bond where M = Cr(II), Mn(II), Fe(II), and Co(II).

Introduction

The reactions of nitric oxide with synthetic metalloporphyrin complexes containing divalent transition metals have been extensively investigated in the last 10 years. Many of these studies have concentrated on Fe(II) porphyrins¹⁻⁹ while nitrosyl

complexes with metalloporphyrins containing central metals other than iron have received less attention in the literature. The nitrosyl complexes of synthetic manganese and chromium

(1) Wayland, B. B.; Olson, L. W. *J. Am. Chem. Soc.* **1974**, *96*, 6037.
(2) Scheidt, W. R.; Frisse, M. E. *J. Am. Chem. Soc.* **1975**, *97*, 17.
(3) Scheidt, W. R.; Picciolo, P. L. *J. Am. Chem. Soc.* **1976**, *98*, 1913.
(4) Buchler, J. W.; Lay, K. L. *Z. Naturforsch., Anorg. Chem., Org. Chem.* **1975**, *30*, 385.

(5) Yoshimura, T. *Arch. Biochem. Biophys.* **1982**, *216*, 625.
(6) Yamamoto, T.; Nozawa, T.; Kaito, A.; Hatano, M. *Bull. Chem. Soc. Jpn.* **1982**, *55*, 2021.
(7) Wayland, B. B.; Minkiewicz, J. V.; Abd-Elmageed, M. E. *J. Am. Chem. Soc.* **1974**, *96*, 2795.
(8) Olson, L. W.; Schaeper, D.; Lançon, D.; Kadish, K. M. *J. Am. Chem. Soc.* **1982**, *104*, 2042.
(9) Lançon, D.; Kadish, K. M. *J. Am. Chem. Soc.* **1983**, *105*, 5610.